WASP-77 Ab: A transiting hot Jupiter planet in a wide binary system.⋆

P. F. L. Maxted[1], D. R. Anderson[1], A. Collier Cameron[2], A. P. Doyle[1], A. Fumel[3], M. Gillon[3], C. Hellier[1], E. Jehin[3], M. Lendl[4], F. Pepe[4], D. L. Pollacco[5,6], D. Queloz[4], D. Ségransan[4], B. Smalley[1], J. K. Southworth [1], A. M. S. Smith[1], A. H. M. J. Triaud[4], S. Udry[4], R. G. West[7],

ABSTRACT

We report the discovery of a transiting planet with an orbital period of 1.36 d orbiting the brighter component of the visual binary star BD −07° 436. The host star, WASP-77 A, is a moderately bright G8 V star (V=10.3) with a metallicity close to solar ([Fe/H]= 0.0 ± 0.1). The companion star, WASP-77 B, is a K-dwarf approximately 2 magnitudes fainter at a separation of approximately 3″. The spectrum of WASP-77 A shows emission in the cores of the Ca II H and K lines indicative of moderate chromospheric activity. The WASP lightcurves show photometric variability with a period of 15.3 days and an amplitude of about 0.3% that is probably due to the magnetic activity of the host star. We use an analysis of the combined photometric and spectroscopic data to derive the mass and radius of the planet ($1.76 \pm 0.06 M_{\rm Jup}$, $1.21 \pm 0.02 R_{\rm Jup}$). The age of WASP-77 A estimated from its rotation rate (~ 1 Gyr) agrees with the age estimated in a similar way for WASP-77 B (~ 0.6 Gyr) but is in poor agreement with the age inferred by comparing its effective temperature and density to stellar models (~ 8 Gyr). Follow-up observations of WASP-77 Ab will make a useful contribution to our understanding of the influence of binarity and host star activity on the properties of hot Jupiters.

Subject headings: Extrasolar planets

[1]Astrophysics Group, Keele University, Staffordshire, ST5 5BG, UK

[2]SUPA, School of Physics and Astronomy, University of St. Andrews, North Haugh, Fife, KY16 9SS, UK

[3]Institut d'Astrophysique et de Géophysique, Université de Liège, Allée du 6 Août, 17, Bat. B5C, Liège 1, Belgium

[4]Observatoire astronomique de l'Université de Genève 51 ch. des Maillettes, 1290 Sauverny, Switzerland

[5]Department of Physics, University of Warwick, Coventry, CV4 7AL

[6]Astrophysics Research Centre, School of Mathematics & Physics, Queen's University, University Road, Belfast, BT7 1NN, UK

[7]Department of Physics and Astronomy, University of Leicester, Leicester, LE1 7RH, UK

⋆Based on observations made with ESO Telescopes at the La Silla Paranal Observatory under programme ID 088.C-0011.

1. Introduction

Ground-based wide-angle surveys such as WASP (Pollacco et al. 2006) and HATnet (Bakos et al. 2004) have now discovered more than 100 transiting hot Jupiter exoplanets around moderately bright stars ($8.5 \lesssim V \lesssim 12.5$). The occurrence rate for hot Jupiters around solar-type stars is known to be about 1% from radial velocity surveys of bright stars (Wright et al. 2012). The transit probability for a typical hot Jupiter with an orbital period ≈ 3 days orbiting a solar-type star is $\approx 10\%$. There are at least 340 000 single FGK-type dwarf stars bright enough to be accessible to survey such as WASP and HATnet (Ammons et al. 2006), so many more transiting hot Jupiters remain to be discovered. Increasing the sample of well-characterised transiting hot Jupiters will clarify relations that may exist between parameters such as period, mass, radius, etc., and so enable us to better understand the formation, evolution and destruction of hot Jupiters (e.g., Matsumura et al. 2010; Knutson et al. 2010; Davis and Wheatley 2009; Batygin et al. 2011). Finding new transiting hot Jupiters will also reveal systems that have extreme properties or unusual configurations that enable them to be characterised in ways not possible for typical hot Jupiters, e.g., low density, bright planets such as WASP-17 that can be characterised by transmission spectroscopy (Wood et al. 2011). Detailed characterisation of a hot Jupiter using ground based observations is always challenging given the small size of the signal due to the secondary eclipse ($\lesssim 0.1\%$) or the variation of transit depth with wavelength ($\lesssim 0.01\%$). Such observations are made easier by the availability of a nearby comparison star that can be used as a comparison source, particularly if the companion is close enough to be included in the same entrance slit for spectroscopic observations (e.g., Sing et al. 2012).

Here we report the discovery by the WASP survey of a companion to the brighter component of the visual binary star BD -07° 436 with a mass $\approx 1.7 M_{\rm Jup}$ and a radius $\approx 1.2 R_{\rm Jup}$. We find that this star (WASP-77 A) is a G8 V star showing moderate chromospheric activity. The planet, WASP-77 Ab, is a typical hot Jupiter planet with an orbital period of 1.36 days. The companion star, WASP-77 B, is a K-dwarf approximately 2 magnitudes fainter then WASP-77 A at a separation of approximately $3''$. We show that this star is physically associated with the star-planet system WASP-77A + WASP-77Ab.

2. Observations

The WASP survey is described in Pollacco et al. (2006) and Wilson et al. (2008) while a discussion of our candidate selection methods can be found in Collier Cameron et al. (2007), Pollacco et al. (2008), and references therein.

The star BD -07° 436 (WASP-77, 1SWASP J022837.22−070338.4) was observed 5594 times by one camera on the WASP-South instrument from 2008 July 30 to 2008 December 12. The synthetic aperture radius used to measure the flux of BD -07° 436 ($48''$) includes the flux from both components of this visual binary star. We selected this star for follow-up observations based

on the characteristics of the periodic transit-like features detected in these data using the detrending and transit detection methods described in Collier Cameron et al. (2007). The transits are also detected with the same period from 3316 observations obtained with the same camera from 2009 August 2 to 2009 December 12. We have also analysed 898 observations obtained with a different camera obtained from 2008 August 18 to 2008 December 25. The WASP photometry is shown as a function of phase for a period of 1.36003 days in Fig. 1.

We obtained 11 radial velocity measurements for WASP-77 A using the fibre-fed CORALIE spectrograph on the Euler 1.2-m telescope located at La Silla, Chile. Details of the instrument and data reduction can be found in Queloz et al. (2000) and Wilson et al. (2008). The RV measurements were performed using cross-correlation against a numerical mask generated from a G2-type star and are given in Table 1, where we also provide the bisector span, BS, which measures the asymmetry of the cross-correlation function. The standard error of the the bisector span measurements is estimated to be $2\sigma_{\rm RV}$. The amplitude and phase of the radial velocity variations and the lack of any significant variation in the bisector span from these data are consistent with the hypothesis that the transit signal in the WASP photometry is due to a planetary mass object. However, the diameter of the entrance aperture to the CORALIE spectrograph ($2''$) is not quite sufficient to completely exclude light from the fainter component contaminating the spectrum of the brighter component and *vice versa*, so the CORALIE data by themselves are not sufficient to exclude the possibility that the transit signal originates from WASP-77 B. We also obtained 4 radial velocity measurements of WASP-77 B with CORALIE, but these are not reported here because the spectra are clearly affected by contamination from the brighter component.

Confirmation that the transit signal originates from the brighter component of BD -07° 436 was obtained using the 60 cm TRAPPIST telescope (Jehin et al. 2011; Gillon et al. 2012) located at ESO La Silla Observatory (Chile). We obtained a sequence of 671 images of BD -07° 436 covering the egress of a transit in good seeing conditions using a z' filter on the night 2011 November 02. From a selection of these images obtained in the best seeing we estimate that the fainter component is 3.22 ± 0.05 times fainter than the brighter component. If the fainter star were responsible for the transit signal in the WASP photometry then the eclipse in the lightcurve of this star would have a depth of about 7%. The stars are not completely resolved in these images, but lightcurves of the two stars obtained using a synthetic aperture with a radius of 3 pixels show a clear transit signal on the brighter component while the fainter component is constant to within 2%. This excludes the possibility that the transit seen in the WASP photometry is due to a deep eclipse in the lightcurve of the fainter component of the visual binary. We observed 3 further transits of BD -07° 436 using TRAPPIST on the nights 2011 November 01 (544 images), 05 November 2011 (1079 images) and 2011 December 01 (925 images). We also obtain a V-band lightcurve on the night 01 November 2011 (327 images) using the EulerCAM instrument on the Euler 1.2-m telescope (Lendl et al. 2012). The flux ratio of the binary in the V-band measured from these images is 5.00 ± 0.13.

We used 8 spectra of WASP-77 A obtained with the HARPS spectrograph on the ESO 3.6m telescope (ESO programme ID 088.C-0011) to confirm that the radial velocity signal seen in our

CORALIE spectra originates from this star and not the fainter component. The entrance aperture to HARPS has a diameter of 1″ and the spectra were all obtained in good seeing so there is negligible contamination of these spectra by light from the fainter component. Radial velocities measured from these spectra using the same method as for our CORALIE spectra are reported in Table 1. Also reported in this table are 4 radial velocities for WASP-77 B measured in the same way. The radial velocity of WASP-77 B is constant to within $10\,\mathrm{m\,s^{-1}}$. The radial velocities of both stars and the bisector span measurements for WASP-77 A are shown as a function of the transit phase in Fig. 2.

We obtained a series of 15,000 images of WASP-77 with an exposure time of 40 milliseconds using the 3-channel photometer ULTRACAM (Dhillon et al. 2007) mounted on the 4.2-m William Herschel Telescope on the night 2012 September 10. The pixel scale is approximately 0.30 arcseconds per pixel and we used the u', g' and r' filters. We then selected 1% of the images in each channel with the best seeing and combined them into three high-resolution images, one for each channel. We used these images to measure the following magnitude difference between the components of the binary: Δu' = 2.961 ± 0.015; Δg' = 2.156 ± 0.004; Δr' = 1.701 ± 0.007. The separation of the components is 3.3 arcseconds. There are no other stars visible in the small images we obtained so we do not have an accurate astrometric solution for the images that we can use to estimate robust errors on this value.

3. Analysis

3.1. Stellar Parameters

Eight individual HARPS spectra of WASP-77 A were co-added to produce a single spectrum with an average S/N of around 80:1. Four co-added HARPS spectra of WASP-77 B yielded a spectrum with an average S/N of 30:1. The standard pipeline reduction products were used in the analysis. The analysis was performed using the methods given in Doyle et al. (2012). The H_α and H_β lines were used to give an initial estimate of the effective temperature ($T_{\rm eff}$). The surface gravity ($\log g$) was determined from the Ca I lines at 6162Å and 6439Å (Bruntt et al. 2010b), along with the Na I D lines. Additional $T_{\rm eff}$ and $\log g$ diagnostics were performed using the Fe lines. An ionisation balance between Fe I and Fe II was required, along with a null dependence of the abundance on either equivalent width or excitation potential (Bruntt et al. 2008). This null dependence was also required to determine the microturbulence ($\xi_{\rm t}$). The parameters obtained from the analysis are listed in Table 2. The elemental abundances were determined from equivalent width measurements of several clean and unblended lines, and additional least squares fitting of lines was performed when required. The quoted error estimates include that given by the uncertainties in $T_{\rm eff}$, $\log g$, and $\xi_{\rm t}$, as well as the scatter due to measurement and atomic data uncertainties.

The projected stellar rotation velocity ($v \sin i_\star$, where $i_\star$ is the inclination of the star's rotation axis) was determined by fitting the profiles of several unblended Fe I lines. For WASP-77 A, a

value for macroturbulence ($v_{\rm mac}$) of 1.7 ± 0.3 km s^{-1} was assumed, based on the calibration by Bruntt et al. (2010a). An instrumental FWHM of 0.04 ± 0.01 Å was determined from the resolution of the spectrograph. A best fitting value of $v \sin i_\star = 4.0 \pm 0.2$ km s^{-1} was obtained for WASP-77 A. For WASP-77 B the macroturbulence was assumed to be zero, since for mid-K stars it is expected to be lower than that of thermal broadening (Gray 2008). A best fitting value of $v \sin i_\star = 2.8 \pm 0.5$ km s^{-1} was obtained for WASP-77 B.

There are emission peaks evident in the Ca II H+K lines of WASP-77 A. The signal-to-noise of the WASP-77 B spectra is too low to discern any emission peaks.

3.2. Rotation period

The WASP lightcurves show a weak, periodic modulation with an amplitude of about 0.3 per cent and a period of about 15 days. This is likely to be a signal of magnetic activity in WASP-77 A caused by star-spots modulating the apparent brightness as the star rotates. WASP-77B may contribute to the variability of the lightcurve on timescales of 10 – 20 d, but it is unlikely to be the source of the 15 day modulation (see Section 3.4). We used the sine-wave fitting method described in Maxted et al. (2011) to refine this estimate of the amplitude and period of the modulation. Variability due to star spots is not expected to be coherent on long timescales as a consequence of the finite lifetime of star-spots and differential rotation in the photosphere so we analysed the two seasons of data separately. We removed the transit signal from the data prior to calculating the periodograms by subtracting a simple transit model from the lightcurve. We calculated periodograms over 4096 uniformly spaced frequencies from 0 to 1.5 cycles/day. The results for the two seasons of data are shown in Fig. 3. The false alarm probability (FAP) levels shown in these figures are calculated using a boot-strap Monte Carlo method also described in Maxted et al. (2011). There is a clear detection of a periodic modulation with a period of 15.09 days in the 2008 data set (FAP=0.006). This is confirmed by a detection at a period of 15.78 days, though with lower significance, in the 2009 data set (FAP=0.052). We adopt a value of $P_{\rm rot} = 15.4 \pm 0.4$ days for the period in the discussion below.

3.3. Mass and radius of WASP-77 Ab

To determine the planetary and orbital parameters, the HARPS radial velocity measurements were combined with the photometry from TRAPPIST and EulerCAM in a simultaneous least-squares fit using the Markov Chain Monte Carlo (MCMC) technique. The details of this process are described in Collier Cameron et al. (2007) and Pollacco et al. (2008). Briefly, the radial velocity data are modelled with a Keplerian orbit and the model of Mandel and Agol (2002) is used to fit the transits in the lightcurves. We used the coefficients from Claret (2000) for the four-coefficient limb-darkening model. We did not include the CORALIE radial velocity data in the least-squares

fit because it is unclear whether they are affected by contamination from the companion star. The TRAPPIST and EulerCAM lightcurves were generated using a synthetic aperture radius large enough to include the light from both stars so we applied a correction for the dilution of the transit depth due to the light from the companion prior to including them in the MCMC analysis.

The baseline of the TRAPPIST and EulerCAM observations is rather short, so we used a measurement of the orbital period from an analysis of the WASP photometry as an additional constraint in the MCMC analysis to the TRAPPIST and EulerCAM data. The parameters of the model are given in Table 3 and the model fits to the lightcurves are shown in Fig. 4. We have assumed that the orbit is circular because the Lucy-Sweeney F-test applied to the results of a least-squares fit for an eccentric orbit (Lucy and Sweeney 1971) shows no evidence for a non-circular orbit ($p = 0.18$, $e = 0.008 \pm 0.005$). The parameters of the transit model and the Keplerian orbit for the host star provide direct estimates for the density of the star and the surface gravity of the planet. To estimate the mass and radius of the planet we require an additional constraint. In this case we derived the following relation specifically for use with WASP-77 A and appropriate for stars with $0.8 < M/M_{\odot} < 1.2$, $-0.8 < [\mathrm{Fe/H}] < 0.3$ and $5000\,\mathrm{K} < T_{\mathrm{eff}} < 6000\,\mathrm{K}$:

$$\log(M/M_{\odot}) = 0.0213 + 1.570\log(T_{\mathrm{eff}}/5781\,\mathrm{K}) + 0.037\log(\rho/\rho_{\odot}) + 0.097[\mathrm{Fe/H}].$$

This equation is the result of a least-squares fit the parameters of 19 stars in eclipsing binary systems with accurately measured masses and radii.[1] The standard deviation of the residuals from the fit is $0.051M_{\odot}$. The standard error estimates for the mass and radius of the star and planet given in Table 3 include this contribution to the error budget.

We created two sets of EulerCAM and TRAPPIST lightcurves where the correction for the dilution was increased or decreased by its standard error and performed an MCMC analysis of these data in the same way as above. The change in the system parameters between these two sets of data was used to estimate the additional uncertainty on the system parameters due to the uncertainty on the dilution factor. The additional uncertainty is found to be small, e.g., the change in $(R_p/R_*)^2$ due to the uncertainty in the dilution factor is 0.00007. This small additional uncertainty is included in the standard errors given for all parameters affected in Table 3.

3.4. Discussion

The density of WASP-77 A derived from our MCMC analysis is independent of any assumption about the evolutionary state of the star, but our estimates for the mass and radius for the planet do assume that the stellar mass derived from the empirical relation above is accurate. To test this assumption we also compared the effective temperature and density of WASP-77 A to the stellar models of Girardi et al. (2000). The results are shown in Fig. 5, where it can be seen the mass

[1] *http://www.astro.keele.ac.uk/jkt/debcat/*

estimated from our MCMC analysis ($M_* = 1.00 \pm 0.05 M_\odot$) is consistent with these stellar models, although the stellar models suggest a slightly lower mass ($\approx 0.89 M_\odot$) and also suggest that the star is rather old (~ 8 Gyr), i.e., slightly evolved. We discuss the reliability of these stellar models further below. The mass and radius of WASP-77 A derived in our MCMC analysis (Table 3) agree well with the mass and radius expected for a main sequence star of the same spectral type (Table 2).

The period of the modulation in the WASP lightcurve together with our estimate for the radius of WASP-77 A implies a rotation velocity $V_{\rm rot} = 3.1 \pm 0.1\,{\rm km\,s^{-1}}$ if we assume that this signal is due to the rotation of this star. This compares with the spectroscopic estimate for the projected rotation velocity $V_{\rm rot} \sin i_\star = 4.0 \pm 0.2\,{\rm km\,s^{-1}}$. The difference between these two values cannot be explained by a mis-alignment between the star's rotation axis and the orbital axis of WASP-77 Ab, but may be explained by an underestimate for the macroturbulence ($v_{\rm mac}$) used in our analysis of the spectrum for WASP-77 A. The calibration of Valenti and Fischer (2005) suggests a value of $v_{\rm mac}$=3.5km s^{-1}. This additional line broadening would reduce the value of $V_{\rm rot} \sin i_\star$ estimated from the spectra sufficiently to make it consistent with the hypothesis that the rotational signal in the WASP lightcurves originates from WASP-77 A. The parameters listed in Table 2 are not affected by this uncertainty in the value of $v_{\rm mac}$. The amplitude of the rotation signal in WASP lightcurves for K-type stars with rotation periods ~ 15 days can be as much a few percent (Collier Cameron et al. 2009) so it also possible that the fainter component of the visual binary contributes to the variability of the lightcurve, but it is unlikely that the modulation of the lightcurve is due to the fainter component alone.

WASP-77 A and WASP-77 B appear to form a genuine physical binary rather than a visual double star. The position angle (PA) and separation of the stars estimated from the images we obtained in good seeing conditions with EulerCAM and TRAPPIST and our high-resolution ULTRACAM images are consistent with the values reported in The Washington Visual Double Star Catalog (WDS 02286−0704; Mason et al. 2001). That catalog reports that 7 observations were obtained between 1930 and 1933, during which time the recorded separation varied from 2.9″ to 3.2″. For comparison, the proper motion of WASP-77 A implies a change of position of 7.8″ between 1930 and 2011. The PA of the binary is $\approx 150^\circ$ whereas the proper motion vector is approximately east-west, so the two components of the binary clearly share a common proper motion.

To estimate the distance to WASP-77, we used a least-squares fit to the data from Boyajian et al. (2012) to establish the following simple relation between the angular diameter ($\theta_{\rm LD}$), H-band magnitude and effective temperature of G-type dwarf stars.

$$\theta_{\rm LD} = 3.206 - 0.679 \log T_{\rm eff} - 0.2{\rm H}$$

We then used this relation together with the radius of WASP-77 A from Table 3 and the apparent H-band magnitude corrected for contribution from the fainter component to estimate a distance $d = 93 \pm 5$ pc. We used the apparent V-band magnitude of WASP-77 (10.30 ± 0.05, Høg et al. 2000) together with the V-band flux ratio measured from our EulerCAM images to estimate an apparent V-band magnitude for WASP-77 B of 12.05±0.06, corresponding to an absolute magnitude

$M_V = 7.2 \pm 0.1$, which is a typical value for a mid-K-type dwarf star (Gray 2008). There is a small difference between the systemic velocity of WASP-77 A and the radial velocity of WASP-77 B ($\approx 1 \mathrm{km\,s^{-1}}$) but this is consistent with the orbital velocity expected for stars of this mass and separation at the estimated distance of the binary.

There is no significant detection of lithium in either WASP-77 A or WASP-77 B. The equivalent width upper limits of 9 mÅ and 13 mÅ, correspond to an abundance upper limit of $\log A(\mathrm{Li}) < 0.76 \pm 0.08$ and $\log A(\mathrm{Li}) < 0.10 \pm 0.14$ respectively. This implies an age at least ∼0.5 Gyr (Sestito and Randich 2005) for both stars.

We can also estimate the ages of WASP-77 A and WASP-77 B based on their rotation periods (gyrochronological age). The values of $v \sin i_\star$ and $R_\star$ for WASP-77A imply a rotation period $P_{\mathrm{rot}} = 14.2 \pm 1.7$ days (assuming $i_\star \approx 90$), which corresponds to a gyrochronological age $\approx 1.0^{+0.5}_{-0.3}$ Gyr using the Barnes (2007) relation. Similarly, an age $\approx 0.4^{+0.3}_{-0.2}$ Gyr is obtained for WASP-77 B from the rotation rate of $P_{\mathrm{rot}} = 12.3 \pm 3.0$ days. These age estimates are clearly incompatible with the age for WASP-77 A we have derived using the stellar models of Girardi et al. (2000). In this case, the agreement between the gyrochronological ages of WASP-77 A and WASP-77 B suggest that gyrochronological age estimates for hot Jupiter host stars are reliable, whereas ages estimated from the effective temperature and density from isochrones may not be. We checked that this is not a specific problem with this particular set of stellar models by estimating the age of WASP-77 A using 5 additional sets of stellar models. The results are shown in Table 4 with stellar models noted as follows: *Claret* (Claret 2005), Y^2 (Demarque et al. 2004), *Teramo* (Pietrinferni et al. 2004), *VRSS* (VandenBerg et al. 2006) and *DSEP* (Dotter et al. 2008). The models and method used are described in more detail in Southworth (2012). It can be seen that stellar models consistently over-estimate the age of WASP-77 A compared to the gyrocronological age. This anomaly may well be related to the poor agreement between the observed radii of some low mass stars and the radii predicted by stellar models, which in-turn is thought to be a related to the rotation and/or magnetic activity in these stars (Kraus et al. 2011; Morales et al. 2010). The mass of the star derived from these stellar models is consistently lower than the value derived from our empirical calibration, although not significantly different. The mass and radius of the planet derived using these stellar models are consistent with the values derived using our empirical calibration.

4. Conclusions

The brighter component of the visual binary star BD −07° 436, WASP-77 A, shows transits every 1.36 days caused by a hot Jupiter companion, WASP-77 Ab, with a mass $\approx 1.8 M_{\mathrm{Jup}}$ and a radius $\approx 1.2 R_{\mathrm{Jup}}$. The radial velocities of the two components of the binary reported here strengthen the conclusion that the two stars are physically associated. The gyrochronological ages for the two stars agree and suggest an age $\sim 0.5 - 1$ Gyr for the stars. If the gyrochronological age for WASP-77 A is correct, then this star has a lower density than predicted by standard stellar

models. This is a phenomenon seen in other stars of similar mass and is likely to be related to the magnetic activity observed in this star.

WASP-South is hosted by the South African Astronomical Observatory and we are grateful for their ongoing support and assistance. Funding for WASP comes from consortium universities and from the UK's Science and Technology Facilities Council. We thank the ULTRACAM team taking the observations of WASP-77 presented here. TRAPPIST is funded by the Belgian Fund for Scientific Research (Fond National de la Recherche Scientifique, FNRS) under the grant FRFC 2.5.594.09.F, with the participation of the Swiss National Science Fundation (SNF). M. Gillon and E. Jehin are FNRS Research Associates.

REFERENCES

Ammons, S. M., Robinson, S. E., Strader, J., Laughlin, G., Fischer, D., and Wolf, A. 2006, ApJ, 638, 1004

Asplund, M., Grevesse, N., Sauval, A. J., and Scott, P. 2009, ARA&A, 47, 481

Bakos, G., Noyes, R. W., Kovács, G., Stanek, K. Z., Sasselov, D. D., and Domsa, I. 2004, PASP, 116, 266

Barnes, S. A. 2007, ApJ, 669, 1167

Batygin, K., Stevenson, D. J., and Bodenheimer, P. H. 2011, ApJ, 738, 1

Boyajian, T. S. et al. 2012, ApJ, 746, 101

Bruntt, H. et al. 2010a, MNRAS, 405, 1907

Bruntt, H., De Cat, P., and Aerts, C. 2008, A&A, 478, 487

Bruntt, H. et al. 2010b, A&A, 519, A51

Claret, A. 2000, A&A, 363, 1081

Claret, A. 2005, A&A, 440, 647

Collier Cameron, A. et al. 2009, MNRAS, 400, 451

Collier Cameron, A. et al. 2007, MNRAS, 380, 1230

Davis, T. A. and Wheatley, P. J. 2009, MNRAS, 396, 1012

Demarque, P., Woo, J.-H., Kim, Y.-C., and Yi, S. K. 2004, ApJS, 155, 667

Dhillon, V. S. et al. 2007, MNRAS, 378, 825

Dotter, A., Chaboyer, B., Jevremović, D., Kostov, V., Baron, E., and Ferguson, J. W. 2008, ApJS, 178, 89

Doyle, A. P., Smalley, B., Maxted, P. F. L., Anderson, D. R., Collier-Cameron, A., Gillon, M., and et al. 2012, MNRAS, submitted.

Gillon, M. et al. 2012, A&A, 542, A4

Girardi, L., Bressan, A., Bertelli, G., and Chiosi, C. 2000, A&AS, 141, 371

Gray, D. F. 2008, The Observation and Analysis of Stellar Photospheres (Cambridge University Press)

Høg, E. et al. 2000, A&A, 355, L27

Jehin, E. et al. 2011, The Messenger, 145, 2

Knutson, H. A., Howard, A. W., and Isaacson, H. 2010, ApJ, 720, 1569

Kraus, A. L., Tucker, R. A., Thompson, M. I., Craine, E. R., and Hillenbrand, L. A. 2011, ApJ, 728, 48

Lendl, M. et al. 2012, A&A, 544, A72

Lucy, L. B. and Sweeney, M. A. 1971, AJ, 76, 544

Mandel, K. and Agol, E. 2002, ApJ, 580, L171

Mason, B. D., Wycoff, G. L., Hartkopf, W. I., Douglass, G. G., and Worley, C. E. 2001, AJ, 122, 3466

Matsumura, S., Peale, S. J., and Rasio, F. A. 2010, ApJ, 725, 1995

Maxted, P. F. L. et al. 2011, PASP, 123, 547

Morales, J. C., Gallardo, J., Ribas, I., Jordi, C., Baraffe, I., and Chabrier, G. 2010, ApJ, 718, 502

Pietrinferni, A., Cassisi, S., Salaris, M., and Castelli, F. 2004, ApJ, 612, 168

Pollacco, D. et al. 2008, MNRAS, 385, 1576

Pollacco, D. L. et al. 2006, PASP, 118, 1407

Queloz, D. et al. 2000, A&A, 354, 99

Sestito, P. and Randich, S. 2005, A&A, 442, 615

Sing, D. K. et al. 2012, arxiv:1208.4982

Southworth, J. 2012, MNRAS, 426, 1291

Valenti, J. A. and Fischer, D. A. 2005, ApJS, 159, 141

VandenBerg, D. A., Bergbusch, P. A., and Dowler, P. D. 2006, ApJS, 162, 375

Wilson, D. M. et al. 2008, ApJ, 675, L113

Wood, P. L., Maxted, P. F. L., Smalley, B., and Iro, N. 2011, MNRAS, 412, 2376

Wright, J. T., Marcy, G. W., Howard, A. W., Johnson, J. A., Morton, T. D., and Fischer, D. A. 2012, ApJ, 753, 160

Table 1: Radial velocity measurements for WASP-77 A and WASP-77 B.

BJD $-2\,450\,000$	RV (km s^{-1})	$\sigma_{\rm RV}$ (km s^{-1})	BS (km s^{-1})
WASP-77 A, CORALIE			
5069.7803	1.3246	0.0049	−0.02828
5163.6091	1.3362	0.0052	−0.04828
5169.6920	1.9673	0.0049	−0.03717
5170.6625	1.5706	0.0053	−0.03203
5188.6258	1.9696	0.0054	−0.04100
5856.7095	1.8655	0.0053	−0.03387
5914.6783	1.7105	0.0043	−0.03349
5915.6775	1.3328	0.0044	−0.02568
5916.6681	1.7087	0.0048	−0.01432
5917.6500	1.9544	0.0047	−0.01638
5918.6645	1.5542	0.0065	−0.01908
WASP-77 A, HARPS			
5832.8615	1.4626	0.0020	0.0365
5832.9040	1.5111	0.0024	0.0352
5832.9110	1.5233	0.0025	0.0410
5889.7458	1.4063	0.0036	0.0307
5890.5370	2.0220	0.0037	0.0375
5890.7386	1.8656	0.0041	0.0180
5891.5721	1.7670	0.0044	0.0260
5891.7468	1.9885	0.0046	0.0432
WASP-77 B, HARPS			
5832.8705	2.7508	0.0047	0.0168
5832.8885	2.7521	0.0061	0.0373
5832.8960	2.7577	0.0063	0.0172
5890.5450	2.7586	0.0057	0.0203

Table 2: Stellar parameters of WASP-77 A and WASP-77 B. Abundances are relative to the solar values obtained by (Asplund et al. 2009).

Parameter	WASP-77 A	WASP-77 B
$T_{\rm eff}$ [K]	5500 ± 80	4700 ± 100
$\log g$	4.33 ± 0.08	4.6 ± 0.15
$\xi_{\rm t}$ [km s^{-1}]	0.8 ± 0.1	
$v \sin i_\star$ [km s^{-1}]	4.0 ± 0.2	2.8 ± 0.5
[Fe/H]	0.00 ± 0.11	−0.12 ± 0.19
[Mg/H]	0.23 ± 0.04	0.09 ± 0.10
[Ca/H]	−0.02 ± 0.13	−0.01 ± 0.13
[Sc/H]	−0.03 ± 0.07	0.14 ± 0.18
[Ti/H]	−0.02 ± 0.10	0.15 ± 0.21
[V/H]	−0.03 ± 0.09	0.39 ± 0.15
[Cr/H]	0.00 ± 0.06	0.07 ± 0.22
[Mn/H]	0.14 ± 0.14	0.06 ± 0.34
[Co/H]	−0.08 ± 0.10	0.24 ± 0.27
[Ni/H]	−0.01 ± 0.08	0.00 ± 0.19
[Y/H]	0.04 ± 0.08	
$\log A$(Li)	$< 0.76\pm$ 0.08	$< 0.10\pm$ 0.14
Mass [$M_\odot$]	1.00 ± 0.07	0.71 ± 0.06
Radius [$R_\odot$]	1.12 ± 0.12	0.69 ± 0.12
Sp. Type[a]	G8	K5

[a]Spectral type estimated from $T_{\rm eff}$ using the table in Gray (2008).

Table 3: System parameters and 1σ error limits derived from the MCMC analysis.

Parameter	Symbol	Value	Units
Orbital period	P	1.3600309 ± 0.0000020	days
Transit epoch	T_0	$2455870.44977 \pm 0.00014$	BJD
Planet/star area ratio	$(R_p/R_*)^2$	0.01693 ± 0.00017	
Transit duration	t_T	0.09000 ± 0.00035	days
Impact parameter	b	$0.06^{+0.07}_{-0.05}$	
Stellar reflex velocity	K_1	0.3219 ± 0.0039	km s^{-1}
Centre-of-mass velocity	γ	1.6845 ± 0.0004	km s^{-1}
Orbital inclination	i	$89.4^{+0.4}_{-0.7}$	$\circ$
Stellar density	ρ_*	$1.157^{+0.016}_{-0.020}$	$\rho_\odot$
Stellar mass	M_*	1.002 ± 0.045	$M_\odot$
Stellar radius	R_*	0.955 ± 0.015	$R_\odot$
Orbital semi-major axis	a	0.0240 ± 0.00036	AU
Planet mass	M_p	1.76 ± 0.06	$M_{\rm Jup}$
Planet radius	R_p	1.21 ± 0.02	$R_{\rm Jup}$[a]
Planet surface gravity	$\log g_p$	3.441 ± 0.008	[cgs]
Planet density	ρ_p	1.00 ± 0.03	$\rho_{\rm Jup}$

[a] $R_{\rm Jup} = 71492\,{\rm km}$

Table 4: Mass, radius and age of WASP-77 A and WASP-77 Ab derived using different sets of stellar models.

	Claret	Y^2	*Teramo*	*VRSS*	*DSEP*
$M_{\rm A}$ ($M_\odot$)	0.948 ± 0.055	0.940 ± 0.048	0.889 ± 0.050	0.893 ± 0.048	0.900 ± 0.008
$R_{\rm A}$ ($R_\odot$)	0.938 ± 0.019	0.935 ± 0.017	0.918 ± 0.018	0.919 ± 0.017	0.922 ± 0.007
$M_{\rm b}$ ($M_{\rm Jup}$)	1.695 ± 0.069	1.686 ± 0.061	1.624 ± 0.064	1.629 ± 0.062	1.637 ± 0.024
$R_{\rm b}$ ($R_{\rm Jup}$)	1.186 ± 0.025	1.183 ± 0.022	1.161 ± 0.024	1.163 ± 0.023	1.166 ± 0.011
Age (Gyr)	$6.8^{+4.7}_{-2.4}$	$5.8^{+2.9}_{-1.8}$	$10.4^{+1.6}_{-4.3}$	$9.5^{+1.6}_{-4.4}$	$8.2^{+0.9}_{-1.6}$

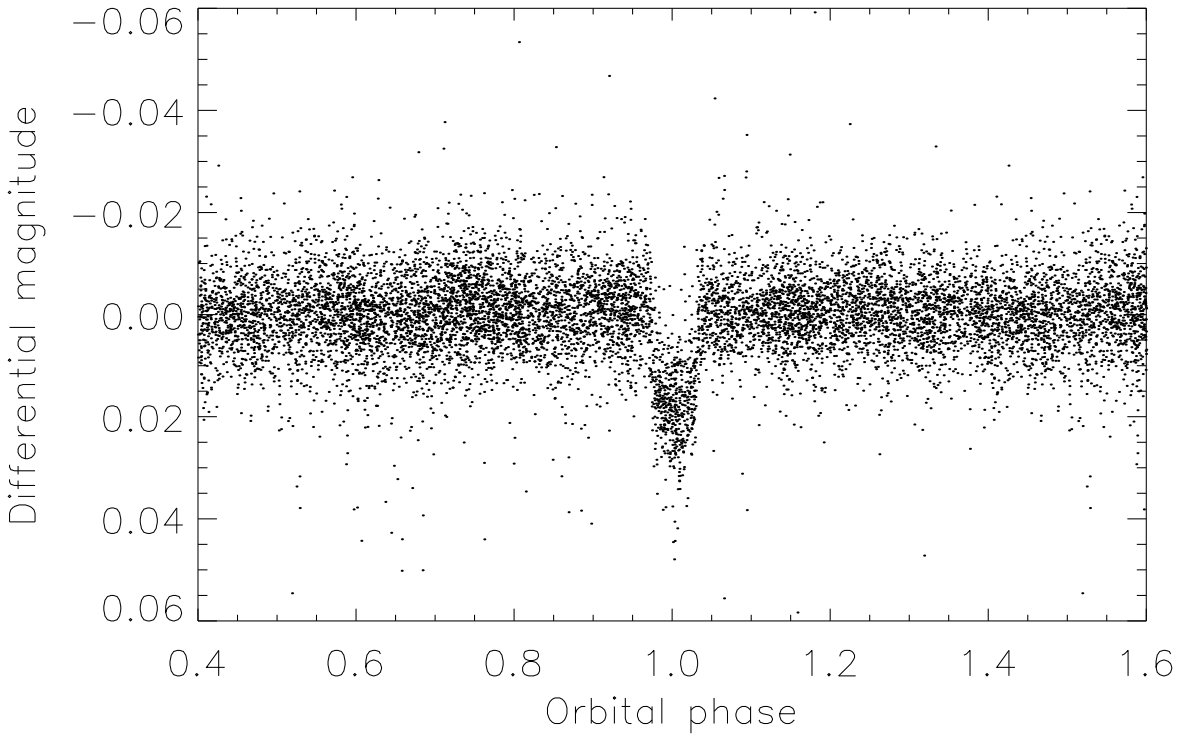

Fig. 1.— WASP photometry of WASP-77 plotted as a function of phase for a period of 1.36003 days.

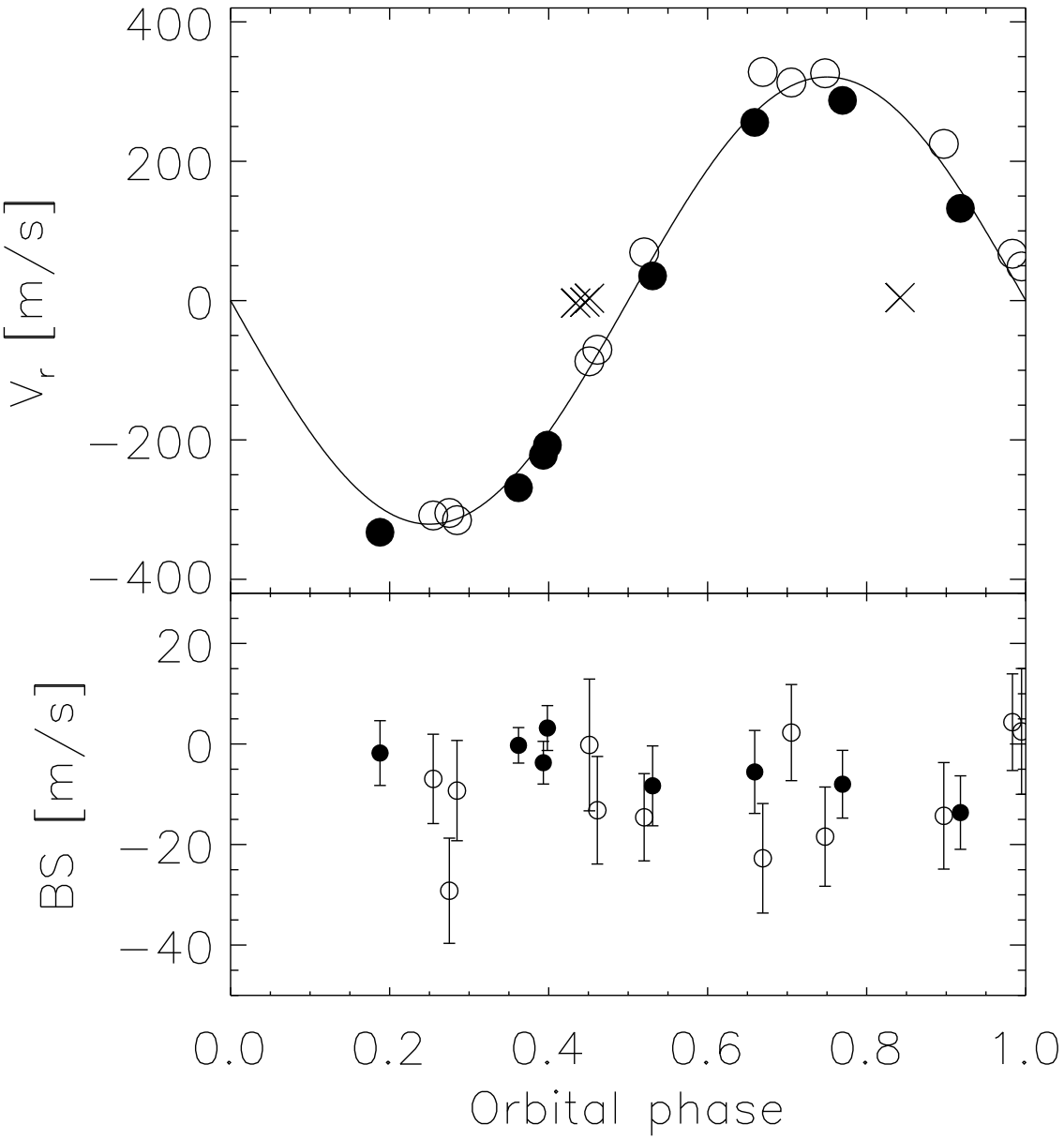

Fig. 2.— Upper panel: Radial velocities of WASP-77 A relative to the centre-of-mass velocity measured using HARPS (filled symbols) and CORALIE (open symbols). Also shown are radial velocities of WASP-77 B relative to their weighted mean value (crosses) and the best-fit circular orbit (solid line) for WASP-77 A. Lower panel: Lower panel: bisector span measurements for WASP-77 A (symbols as in upper panel).

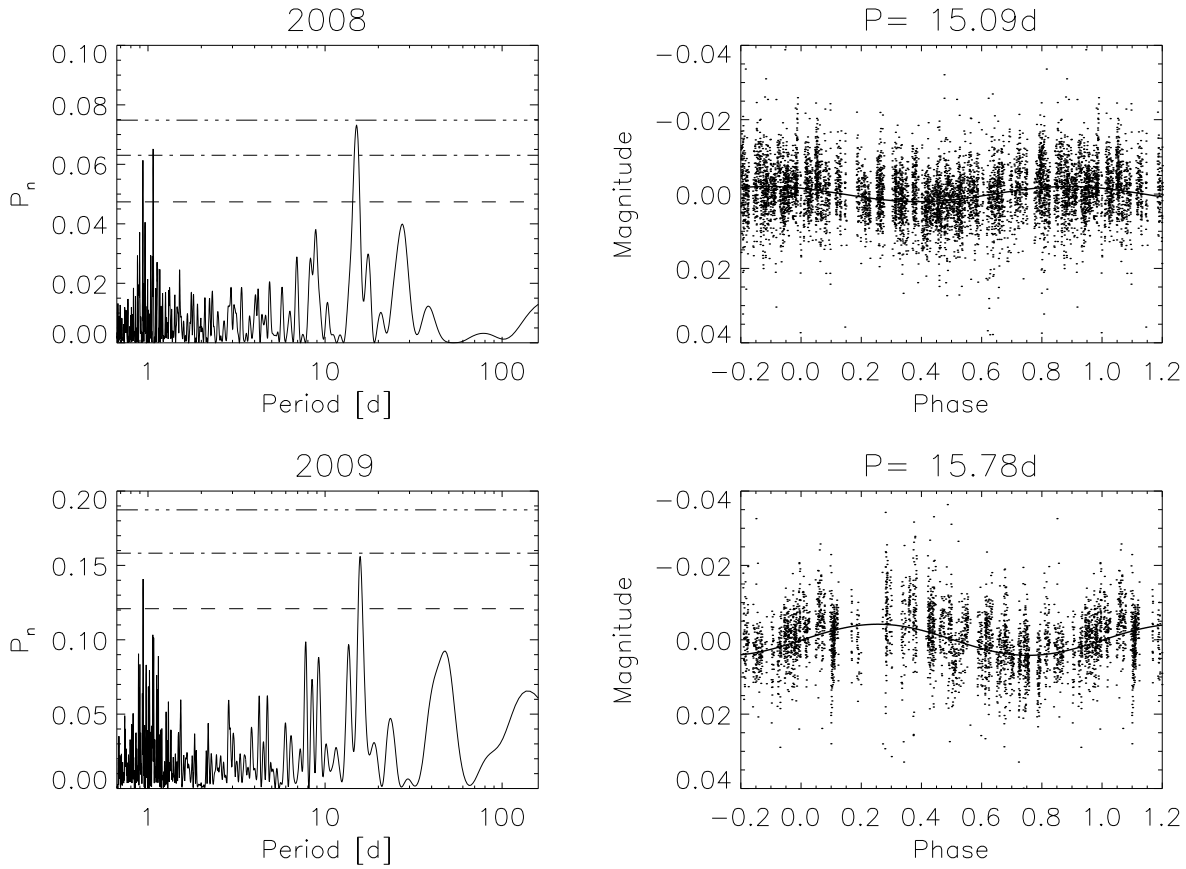

Fig. 3.— *Left panels* Periodograms for the WASP data from two different observing seasons for WASP-77. Horizontal lines indicate false alarm probability levels FAP=0.1,0.01,0.001. The year of observation is noted in the title to each panel. *Right panels* Lightcurves folded on the best period as noted in the title.

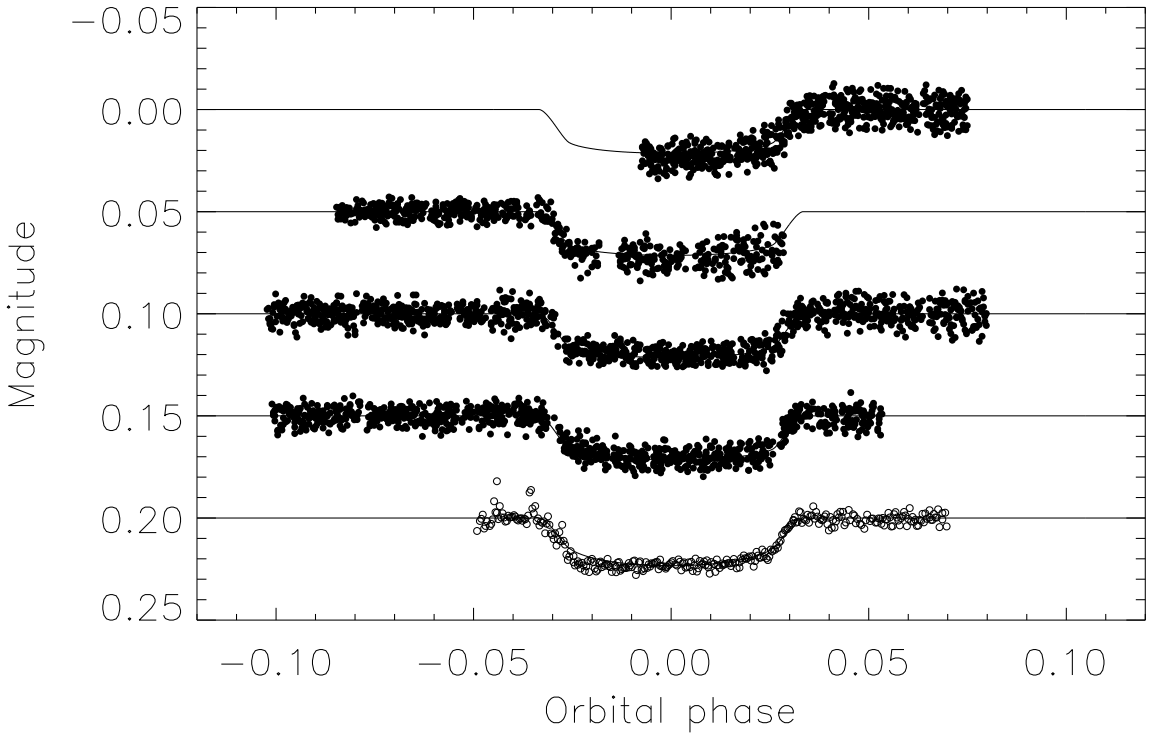

Fig. 4.— Photometry of WASP-77 A corrected for the dilution due to WASP-77 B. Data from TRAPPIST are plotted with filled circles in date order from top-to-botton. EulerCAM data are shown with open circles. The solid line shows the lightcurve model for the parameters in Table 3.

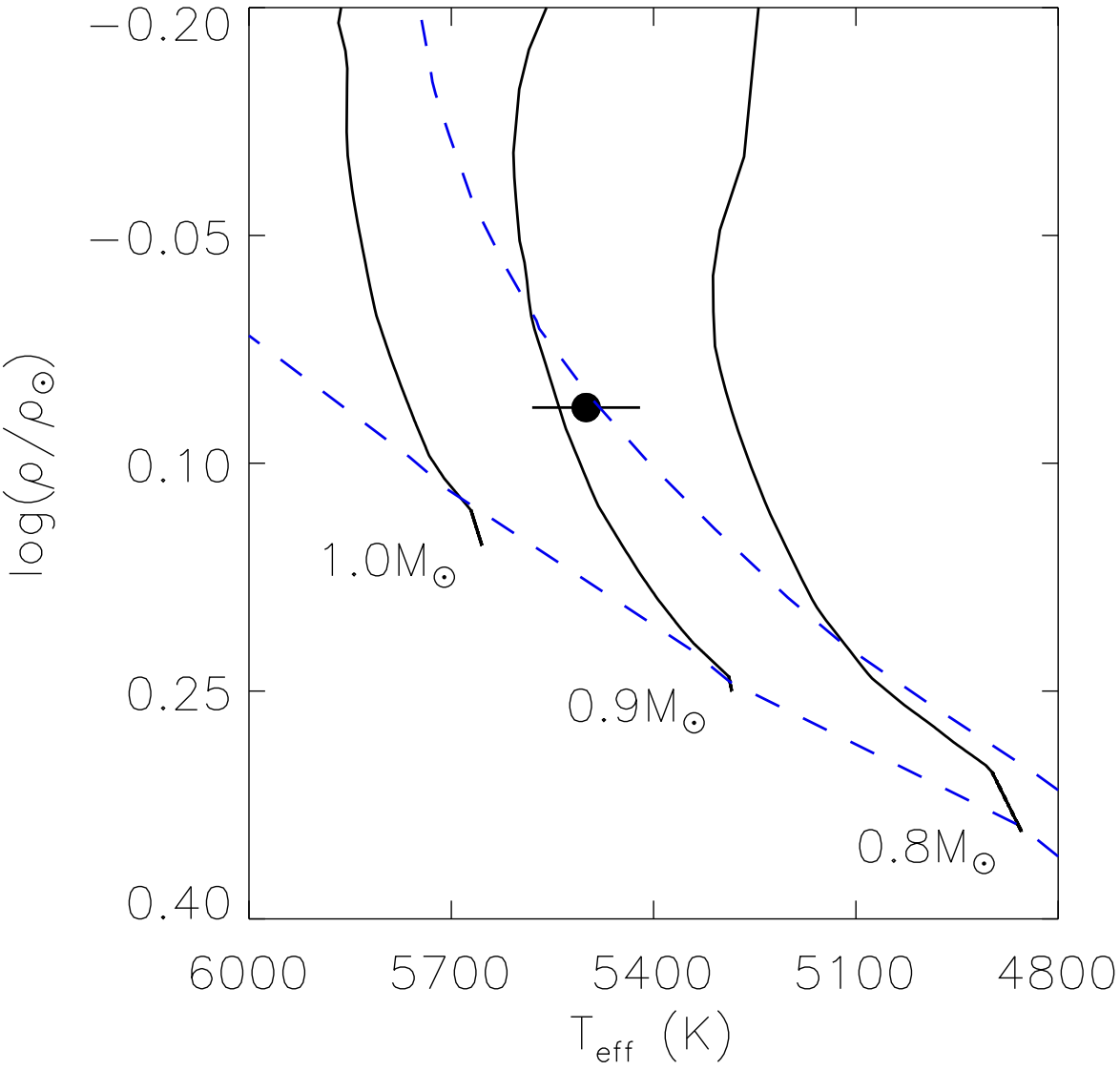

Fig. 5.— Comparison of the effective temperature and stellar density of WASP-77 A to the stellar models of Girardi et al. (2000). Dashed lines show isochrones for age of 10 Myr and 10 Gyr. Solid lines are evolutionary tracks for stellar masses as indicated.